This article was downloaded by: *[Nali, Pietro]*
On: *8 November 2010*
Access details: *Access Details: [subscription number 929202985]*
Publisher *Taylor & Francis*
Informa Ltd Registered in England and Wales Registered Number: 1072954 Registered office: Mortimer House, 37-41 Mortimer Street, London W1T 3JH, UK

International Journal for Computational Methods in Engineering Science and Mechanics
Publication details, including instructions for authors and subscription information:
http://www.informaworld.com/smpp/title~content=t713872093

A Comparison of Various Two-Dimensional Assumptions in Finite Element Analysis of Multilayered Plates

E. Carrera[a]; A. Büttner[b]; J. P. Nalif[b]; T. Wallmerperger[c]; B. Kröplin[c]
[a] Aerospace Department, Politecnico di Torino, Torino, Italy [b] Aerospace Engineering, University of Stuttgart (Institut für Statik und Dynamik der Luft- und Raumfahrttechnik), Stuttgart, Germany [c] Institut für Statik und Dynamik der Luft- und Raumfahrttechnik, Stuttgart, Germany

Online publication date: 06 November 2010

To cite this Article Carrera, E. , Büttner, A. , Nalif, J. P. , Wallmerperger, T. and Kröplin, B.(2010) 'A Comparison of Various Two-Dimensional Assumptions in Finite Element Analysis of Multilayered Plates', International Journal for Computational Methods in Engineering Science and Mechanics, 11: 6, 313 — 327
To link to this Article: DOI: 10.1080/15502287.2010.516790
URL: http://dx.doi.org/10.1080/15502287.2010.516790

PLEASE SCROLL DOWN FOR ARTICLE

Full terms and conditions of use: http://www.informaworld.com/terms-and-conditions-of-access.pdf

This article may be used for research, teaching and private study purposes. Any substantial or systematic reproduction, re-distribution, re-selling, loan or sub-licensing, systematic supply or distribution in any form to anyone is expressly forbidden.

The publisher does not give any warranty express or implied or make any representation that the contents will be complete or accurate or up to date. The accuracy of any instructions, formulae and drug doses should be independently verified with primary sources. The publisher shall not be liable for any loss, actions, claims, proceedings, demand or costs or damages whatsoever or howsoever caused arising directly or indirectly in connection with or arising out of the use of this material.

International Journal for Computational Methods in Engineering Science and Mechanics, 11:313–327, 2010
Copyright © Taylor & Francis Group, LLC
ISSN: 1550–2287 print / 1550–2295 online
DOI: 10.1080/15502287.2010.516790

Taylor & Francis
Taylor & Francis Group

A Comparison of Various Two-Dimensional Assumptions in Finite Element Analysis of Multilayered Plates

E. Carrera,[1] A. Büttner,[2] J. P. Nalif,[2] T. Wallmerperger,[3] and B. Kröplin[3]

[1]*Aerospace Department, Politecnico di Torino, Torino, Italy*
[2]*Aerospace Engineering at the University of Stuttgart (Institut für Statik und Dynamik der Luft- und Raumfahrttechnik), Stuttgart, Germany*
[3]*Institut für Statik und Dynamik der Luft- und Raumfahrttechnik, Stuttgart, Germany*

Downloaded By: [Nali, Pietro] At: 11:45 8 November 2010

This work deals with a refined Finite Element (FE) analysis of multilayered plates. Various two-dimensional axiomatic assumptions in the thickness direction are illustrated and discussed by considering: 1-Taylor type expansion; 2-combinations of Legendre polynomials; 3-Lagrange polynomials. Both cases of an equivalent single layer description (the whole plate is seen as an equivalent single layer) and a layer-wise description (each layer is seen as an independent plate) have been implemented. The order N of the thickness expansions is a free parameter of the present formulation. A large variety of plate theories are therefore obtained. Related standard serendipity-type quadrilateral FEs are considered in this paper. FE matrices are written in a concise form by referring to the Carrera Unified Formulation and in terms of a few fundamental nuclei, whose form does not depend on the through-the-thickness polynomial assumption, order N, variable description or element number of nodes. The advantages and disadvantages of the various FEs are discussed by considering static and dynamic problems related to significant multilayered plate problems.

Keywords Plate modeling, finite elements, CUF, thickness assumptions, layer wise description

1. INTRODUCTION

Layered or multilayered structures are being increasingly employed in the aerospace, ship and automotive industries. Early examples of layered structures are sandwich structures which consist of three layers (two skin layers with a soft core layer in between) [1] as well as thermal protection systems (two layers of different metals or metal-ceramic materials) [2]. More recent applications of multilayered structures consist of laminated structures made of composite materials (with carbon, glass, boron or metallic fibers): layers of the same/different materials are placed (according to a given stacking sequence of fiber orientation) one over the other to obtain a laminated structure. In the case of axialsymmetric structures, such as pressure vessels, the filament winding technique is preferred [3]. Smart structures with piezoelectric layers or patches embedded on the inside represent another example of multilayered structures [4]. Single-walled and multi-walled nanotubes can be considered as advanced present/future multilayered structures [5] as far as classical "one-layered" plates are considered, the multilayered ones present some complicating effects due to their intrinsic transverse and in-plane strong anisotropy.

These structures are often constituted by the assembly of flat or curved panels. The use of computational methods is mandatory to analyze anisotropic multilayered plates/shells. In the case of thermal protection systems and smart structures, the complexity increases due to coupling interactions among the mechanical, thermal and electric fields. The Finite Element Method (FEM) represents a well established technique that can solve structural problems in both linear and nonlinear cases. The present paper is focused on linear multilayered plate problems with pure mechanical loading. Many research works have been devoted to the appropriate modeling of multilayered structures and to fulfill the so called (C_z^0-Requirements [6] in the last three decades: the displacement and transverse stress variables must be a C0-function in the z-thickness-direction. Due to transverse material discontinuity at the layer interfaces, the continuity is in general not guaranteed for transverse stress variables. In other words a Zig-Zag (ZZ) form of displacement components and Interlaminar Continuity (1C) of transverse shear and normal stress is not guaranteed by classical modeling such as the Classical Lamination Theory, CLT (based on Kirchhoff type assumptions [7]), or the First order Shear Deformation Theory, FSDT (based

Address correspondence to E. Carrera, Professor of Aerospace Structures and Computational Aeroelasticity, Aerospace Department, Politecnico di Torino, Corso Ducadegli Abruzzi 24, 10129 Torino, Italy, E-mail: erasmo.carrera@polito.it, Website: www.mu12.com

on Reissner-Mindlin type assumption [8]). Among the available review papers, those in [8–12] are herein mentioned. Additional contributions on higher order theories for the analysis of layered composite plates are proposed in works [13–18]. The historical note on Zig-Zag theories in [19] is particularly recommended to highlight some of the most relevant contributions from the Russian literature.

In the framework of axiomatic theories with displacement unknowns formulations, two-dimensional models for laminated plates can be formulated according to the following two points:

1. a two-dimensional expansion is made for the unknown variables u_τ in the in-plane domain $x - y$. The out-of-plane behavior is modeled according to a given set of thickness functions $F_\tau(z)$:

$$u(x, y, z) = F_\tau(z)u_\tau(x, y), \quad \tau = 0, N. \tag{1}$$

2. the assumption in Eq. (l) can be made at a layer or at a multilayer level, obtaining the so called Layer-Wise (LW) and Equivalent Single Layer (ESL) modeling, respectively.

The present work is devoted to a comparison between several plate Finite Elements (FEs) obtained with different choices of thickness functions $F_\tau(z)$. Both LW or ESL modelings are addressed. The following choices are considered for the base functions $F_\tau(z)$:

1. Taylor type expansion in terms of power of z;
2. Combinations of Legendre polynomials;
3. Lagrange polynomials.

The first case is the best known and most frequently considered in the open literature (see the above mentioned review articles). The other two cases are convenient in the case of LW variable descriptions since they "naturally" lead to a ZZ-form of displacement through the thickness of the multilayered plate [19, 20]. In particular, the use of Lagrange polynomials leads to a finite element formulation with pure displacement variables as the primary unknowns. Such a property can be convenient to develop nonlinear formulations since the related rigid body motion leads to the zero-strain condition [21].

Isoparametric FEs have been developed in this work. The main objective is to discuss the following point: what is the most accurate approach (the most appropriate combination of LW or ESL description with Taylor, Legendre or Lagrange polynomials) versus computational costs (number of Degrees Of Freedoms DOFs) for a given problem?

Previous works have here been extended for this purpose [22–24]. In particular, with respect to existing works, the present paper contributes: by formulating FEs using Lagrange polynomials in both ESL and LW modeling cases; by extending the use of Legendre polynomials to an ESL description.

The order of the expansion N is considered in all cases as a free parameter of the investigation. All the above modellings are implemented by referring to the Carrera Unified Formulation CUF [25, 26]. Such a formulation permits one to obtain the FE matrices in terms of fundamental nuclei whose form is independent of the choice of the thickness functions $F_\tau(z)$, order, element number of nodes as well as of the variable description (ESL, LW).

The paper has been organized as it follows. Sec. 2 discusses the various two-dimensional plate theories based on different thickness functions $F_\tau(z)$ (Talyor, Legendre, Lagrange polynomials). The constitutive equations and geometrical relations are listed in Sec. 3. The FE matrices are obtained in Sec. 4. FEM static and dynamic problems are described in Sec. 5. The numerical results are discussed in Sec. 5. The conclusions are provided in Sec. 6.

2. CONSIDERED PLATE THEORIES BASED ON CUF

2.1. Main idea of the Carrera Unified Formulation

The main idea of the CUF consists of using a generalized expansion for the unknowns in the thickness direction, based on an set of functions, called thickness functions. In this way, the three-dimensional problem of multilayered plates can be reduced to a two-dimensional problem. According to the CUF, the displacement field (or more in general the primary unknowns) can be written as follows.

$$\boldsymbol{u}(x, y, z) = F_\tau(z)\boldsymbol{u}_\tau(x, y) = F_\tau \boldsymbol{u}_\tau, \quad \tau = 1, \ldots, N + 1. \tag{2}$$

where

A cartesian reference system is considered, where z is the the out-of-plane axis. F_τ is now the set of the thickness functions and N is the order of the expansion. With this formulation two different descriptions along the thickness are possible for the unknowns: ESL and LW (see Fig. 1). Governing equations can be obtained according to a chosen variational statement and the resulting matrices are not affected neither on. the chosen theory (ESL or LW) nor on the polynomial expansion order.

2.2. Different Thickness Polynomials for LW Description

The thickness expansion is considered separately for each layer with a LW model. As a consequence, displacement variables are assumed independently for each layer. The interlaminar continuity of the displacements can be imposed at each interface between layers by the assembly procedure. The generalized displacement assumptions of the k-th layer (superscript k) can be stated as

$$\boldsymbol{u}^k = F_t \boldsymbol{u}_t^k + F_b \boldsymbol{u}_b^k + F_r \boldsymbol{u}_r^k = F_\tau \boldsymbol{u}_\tau^k, \tag{3}$$

where $\tau = t, b, r; \quad r = 2, 3, \ldots, N$ and $k = 1, 2, \ldots, N_L$.

Downloaded By: [Nali, Pietro] At: 11:45 8 November 2010

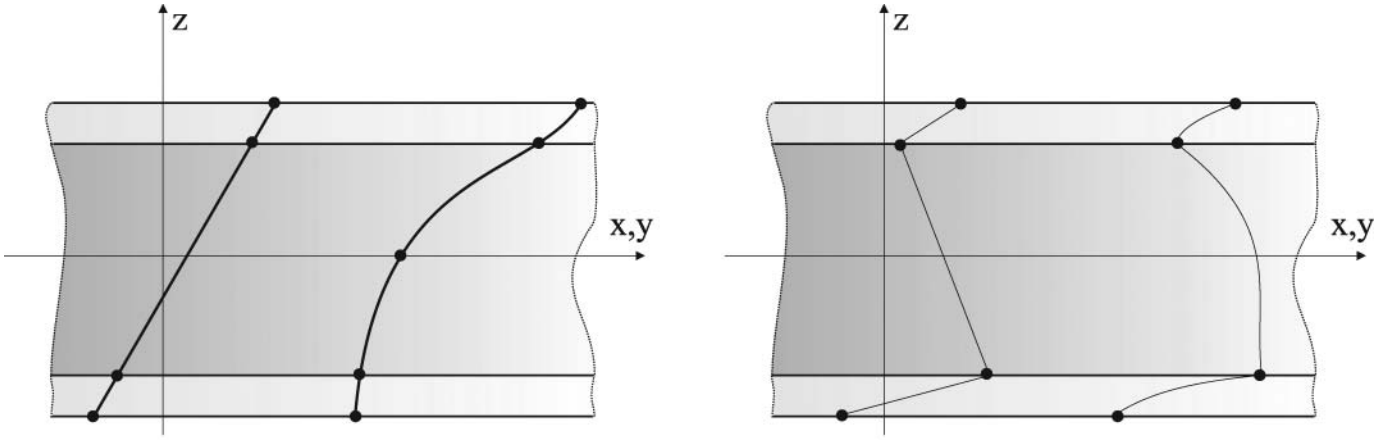

(a) Linear and cubic ESL analysis (b) Linear and cubic LW analysis

FIG. 1. Qualitative unknowns description for a three layered structure in case of ESL (a) and LW (b) modeling.

Downloaded By: [Nali, Pietro] At: 11:45 8 November 2010

The role of index τ in Eq. 2 is covered by index t, b, r in Eq. 3 in order to provide a more clear notation. The displacement variables $\boldsymbol{u}_t^k$ and $\boldsymbol{u}_b^k$ are the values related to the top and bottom surface of the k-layer. The interlaminar continuity condition leads to

$$\boldsymbol{u}_t^k = \boldsymbol{u}_b^{(k+1)}, \quad \text{with} \quad k = 1, \ldots, N_L - 1. \tag{4}$$

2.2.1. Legendre Polynomials

For the thickness functions F_τ a combinations of Legendre polynomials $P_j = P_j(\zeta_k)$ can be used, wherein ζ_k shall be the dimensionless thickness coordinate of the layer k defined in the domain $-1 \leq \zeta_k \leq 1$. The Legendre Polynomials up to 4-th order are given below.

$$P_0 = 1 \quad P_1 = \zeta_k \quad P_2 = 3/2\left(\zeta_k^2 - 1\right) \quad P_3 = 5/2\ \zeta_k^3 - 3/2\ \zeta_k$$
$$P_4 = 35/8\ \zeta_k^4 - 15/4\ \zeta_k^2 + 3/8$$

The following combinations of P_j are chosen as thickness functions F_τ in order to make the top and bottom primary unknowns coincident with $\boldsymbol{u}_b^k$ and $\boldsymbol{u}_t^k$ displacements, respectively.

$$F_t = (P_0 + P_1)/2; \quad F_b = (P_0 - P_1)/2;$$
$$F_r = P_r - P_{r-2}, \quad \text{with} \quad r = 2, 3, \ldots, N.$$

The following properties are respected:

$$\zeta_k = 1 : F_t = 1; \quad F_r = 0; \quad F_b = 0;$$
$$\zeta_k = -1 : F_t = 0; \quad F_r = 0; \quad F_b = 1.$$

2.2.2. Lagrange Polynomials

The use of Lagrange polynomials for the expansion of primary unknowns through the plate-thickness direction is proposed. The Lagrange polynomials defined in the domain $[-1, 1]$ are presented in Tab. 1 up to the 4-th order and unless otherwise noted, the parameters z_i for higher order Lagrange polynomials divide the domain $[-1, 1]$ in equal distances, i.e. for the 4-th order case:

$$\zeta_k(z_1) = -0.5; \quad \zeta_k(z_2) = 0.0; \quad \zeta_k(z_3) = 0.5;$$

As in the case of Legendre polynomials, the two Lagrange polynomials Ft and F_b refer to the top and bottom surface of each layer.

TABLE 1
Thickness functions -$F_\tau(\zeta)$ with Lagrange polynomials up to 4th order

1st order
$F_t = (1 + \zeta)/2$
$F_b = (1 - \zeta)/2$
2nd order
$F_t = -(1 + \zeta)(\zeta - z_1)/(2(-1 + z_1))$
$F_2 = (-1 + \zeta^2)/(-1 + z_1^2)$
$F_b = (-1 + \zeta)(\zeta - z_1)/(2(1 + z_1))$
3rd order
$F_t = (1 + \zeta)(\zeta - z_1)(\zeta - z_2)/(2(-1 + z_1)(-1 + z_2))$
$F_2 = -(-1 + \zeta)(1 + \zeta)(\zeta - z_1)/((z_1 - z_2)(-1 + z_2^2))$
$F_3 = (-1 + \zeta)(1 + \zeta)(\zeta - z_2)/((-1 + z_1^2)(z_1 - z_2))$
$F_b = -(-1 + \zeta)(\zeta - z_1)(\zeta - z_2)/(2(1 + z_1)(1 + z_2))$
4th order
$F_t = -(1 + \zeta)(\zeta - z_1)(\zeta - z_2)(\zeta - z_3)\ /$
$(2(-1 + z_1)(-1 + z_2)(-1 + z_3))$
$F_2 = (-1 + \zeta)(1 + \zeta)(\zeta - z_1)(\zeta - z_2)/$
$((z_1 - z_3)(z_2 - z_3)(-1 + z_3^2))$
$F_3 = -(-1 + \zeta)(1 + \zeta)(\zeta - z_1)(\zeta - z_3)/$
$((z_1 - z_2)(-1 + z_2^2)(z_2 - z_3))$
$F_4 = (-1 + \zeta)(1 + \zeta)(\zeta - z_2)(\zeta - z_3)/$
$((-1 + z_1^2)(z_1 - z_2)(z_1 - z_3))$
$F_b = (-1 + \zeta)(\zeta - z_1)(\zeta - z_2)(\zeta - z_3)/$
$(2(1 + z_1)(1 + z_2)(1 + z_3))$

2.3. Thickness Polynomials for ESL Description

In ESL theory, a global assumption for primary unknowns is considered along the plate thickness (the whole multilayered plate is modeled as an Equivalent-Single-Layer plate). A Taylor expansion assumption is commonly found in literature. Other polynomial choices are possible: Lagrange or Legendre polynomials described in Sec. 2.2 can be considered as an alternative. In case of Taylor expansion:

$$F_b = 1, \quad F_r = z^r, \quad F_t = z^N, \quad r = 1, 2, \ldots, N-1. \tag{5}$$

If a taylor expansion is addressed to, the subscript b denotes values related to the plate reference surface Ω, while subscript t is related to the highest order term.

3. CONSTITUTIVE EQUATIONS AND GEOMETRIC RELATIONS

The general material behavior is described by the Hooke's law: the six stress component $\boldsymbol{\sigma}$ are related to the six strain component $\boldsymbol{\epsilon}$ via the elastic stiffness coefficients in matrix $\tilde{\boldsymbol{C}}$. Stresses and strains are split in in-plane and transverse components denoted with the subscript p and n respectively:

$$\begin{aligned} \boldsymbol{\sigma}_p &= [\sigma_{11},\ \sigma_{22},\ \sigma_{12}]^T; \quad & \boldsymbol{\sigma}_n &= [\sigma_{13},\ \sigma_{23},\ \sigma_{33}]^T; \\ \boldsymbol{\epsilon}_p &= [\epsilon_{11},\ \epsilon_{22},\ \epsilon_{12}]^T; \quad & \boldsymbol{\epsilon}_n &= [\epsilon_{13},\ \epsilon_{23},\ \epsilon_{33}]^T. \end{aligned} \tag{6}$$

Subscripts 1 and 2 indicate the in-plane axes. Axis 3 concerns the out-of-plane direction. Superscript T indicates the transposition of the vector/matrix.
According to the above partitioning, the Hooke's law states:

$$\begin{aligned} \boldsymbol{\sigma}_p &= \boldsymbol{C}_{pp}\boldsymbol{\epsilon}_p + \boldsymbol{C}_{pn}\boldsymbol{\epsilon}_n; \\ \boldsymbol{\sigma}_n &= \boldsymbol{C}_{np}\boldsymbol{\epsilon}_p + \boldsymbol{C}_{nn}\boldsymbol{\epsilon}_n. \end{aligned} \tag{7}$$

The arrays of the elastic material properties for monoclinic behavior take the following explicit form:

$$\tilde{\boldsymbol{C}}_{pp} = \begin{bmatrix} C_{11} & C_{12} & C_{16} \\ C_{12} & C_{22} & C_{26} \\ C_{16} & C_{26} & C_{66} \end{bmatrix}; \quad \tilde{\boldsymbol{C}}_{pn} = \begin{bmatrix} 0 & 0 & C_{13} \\ 0 & 0 & C_{23} \\ 0 & 0 & C_{36} \end{bmatrix};$$

$$\tilde{\boldsymbol{C}}_{np} = \begin{bmatrix} 0 & 0 & 0 \\ 0 & 0 & 0 \\ \tilde{C}_{13} & \tilde{C}_{23} & \tilde{C}_{36} \end{bmatrix}; \ \tilde{\boldsymbol{C}}_{nn} = \begin{bmatrix} C_{55} & C_{45} & 0 \\ C_{45} & C_{44} & 0 \\ 0 & 0 & C_{33} \end{bmatrix}.$$

The geometric relations in linearized form are employed to express the strains $\boldsymbol{\epsilon}_p$ and $\boldsymbol{\epsilon}_n$ in terms of the displacements components in vector $\boldsymbol{u} = [u_x, u_y, u_z]^T$:

$$\boldsymbol{\epsilon}_p = \boldsymbol{D}_p\boldsymbol{u}; \quad \boldsymbol{\epsilon}_n = \boldsymbol{D}_n\boldsymbol{u}. \tag{8}$$

The arrays $\boldsymbol{D}_p$ and $\boldsymbol{D}_n$ contain the differential operators. Their explicit form is:

$$\boldsymbol{D}_p = \begin{bmatrix} \partial_x & 0 & 0 \\ 0 & \partial_y & 0 \\ \partial_y & \partial_x & 0 \end{bmatrix}; \quad \boldsymbol{D}_n = \begin{bmatrix} \partial_x & 0 & \partial_x \\ 0 & \partial_z & \partial_y \\ 0 & 0 & \partial_z \end{bmatrix}.$$

The differential operator array $\boldsymbol{D}_n$ can be split in in-plane and out-of-plane contributions:

$$\boldsymbol{D}_n = \boldsymbol{D}_{n\Omega} + \boldsymbol{D}_{nz}, \tag{9}$$

with:

$$\boldsymbol{D}_{n\Omega} = \begin{bmatrix} 0 & 0 & \partial_x \\ 0 & 0 & \partial_y \\ 0 & 0 & 0 \end{bmatrix}; \quad \boldsymbol{D}_{nz} = \begin{bmatrix} \partial_z & 0 & 0 \\ 0 & \partial_z & 0 \\ 0 & 0 & \partial_z \end{bmatrix}.$$

4. FINITE ELEMENT MATRICES

An exhaustive description of the derivation of FE matrices can be found in [23, 26]. According to CUF, the fundamental nuclei are independent of the type of polynomials employed for the through-the-thickness expansion. As a consequence, the fundamental nuclei related to the use of the various polynomial sets proposed in this paper, are "formally" coincident to those illustrated in [23]. For sake of completeness the fundamental nuclei are obtained in the following section.

4.1. FE Discretization

If the Finite Element Method (FEM) is employed, the primary unknowns $\boldsymbol{u}_\tau$ can be expressed in terms of their nodal values $\boldsymbol{q}_\tau$. That is discretized via the shape functions N_i:

$$\boldsymbol{u}_\tau^k(x, y) = N_i(x, y)\boldsymbol{q}_{\tau i}^k \quad i = 1, 2, \ldots, N_n. \tag{10}$$

N_n denotes the number of nodes concerning the considered finite element and $\boldsymbol{q}_{\tau i}^k$ is the vector of nodal unknowns.

$$\boldsymbol{q}_{\tau i}^k = [q_{u_x\tau i}, q_{u_y\tau i}, q_{u_z\tau i}]^T \tag{11}$$

Substituting Eq. (10) in Eq. (2), the final three-dimensional expression of the displacements field is obtained:

$$\boldsymbol{u}^k(x, y, z) = F_\tau(z)N_i(x, y)\boldsymbol{q}_{\tau i}^k. \tag{12}$$

4.2. FE Fundamental Nuclei

The Principle of Virtual Displacements (PVD) application for a multilayered plate takes the following form:

$$\sum_{k=1}^{N_L} \int_{\Omega_k} \int_{h_k} \left(\delta\boldsymbol{\epsilon}_p^{k^T}\boldsymbol{\sigma}_p^k + \delta\boldsymbol{\epsilon}_n^{k^T}\boldsymbol{\sigma}_n^k\right) d\Omega_k \quad dz = \delta L_e - \delta L_{in}, \tag{13}$$

Downloaded By: [Nali, Pietro] At: 11:45 8 November 2010

Downloaded By: [Nali, Pietro] At: 11:45 8 November 2010

where δ is the variational symbol and h_k is the thickness of the k-th layer. The left part represents the mechanical internal work L_i while L_e and L_{in} are the work made by external and inertial loads, respectively. The virtual variation of the external work can be expressed as:

$$\delta L_e = \int_\Omega (\delta \boldsymbol{u}^T \bar{\boldsymbol{t}}) d\Omega, \tag{14}$$

where $\bar{\boldsymbol{t}}$ is the mechanical loading vector of applied pressure. The expression of the virtual variation of the inertial load is:

$$\delta L_{in} = \int_v (\delta \boldsymbol{u}^T \rho \ddot{\boldsymbol{u}}) dV, \tag{15}$$

where $\ddot{\boldsymbol{u}}$ is the second derivative of the displacement $\boldsymbol{u}$ with respect to time.

Restricting Eq. (13) to the layer k and by introducing Hooke's law in Eq. (7) it becomes:

$$\int_{\Omega_k}\int_{h_k} \left[\delta\boldsymbol{\epsilon}_p^{k^T}\left(\tilde{\boldsymbol{C}}_{pp}^k\boldsymbol{\epsilon}_p^k + \tilde{\boldsymbol{C}}_{pn}^k\boldsymbol{\epsilon}_n^k\right) + \delta\boldsymbol{\epsilon}_n^{k^T}\left(\tilde{\boldsymbol{C}}_{np}^k\boldsymbol{\epsilon}_p^k + \tilde{\boldsymbol{C}}_{nn}^k\boldsymbol{\epsilon}_n^k\right)\right] d\Omega_k \quad dz = \delta L_e^k - \delta L_{in}^k. \tag{16}$$

Considering the thickness expansion in Eq. (2), the geometrical relations collected in the differential operator in Eq. (9) as well as the finite element discretization in Eq. (10), the strains $\boldsymbol{\epsilon}_p$ and $\boldsymbol{\epsilon}_n$ can be written as follows.

$$\boldsymbol{\epsilon}_p^k = F_\tau \boldsymbol{D}_p(N_i\boldsymbol{I})\boldsymbol{q}_{\tau i}^k \tag{17}$$

$$\boldsymbol{\epsilon}_n^k = F_\tau \boldsymbol{D}_{n\Omega}(N_i\boldsymbol{I})\boldsymbol{q}_{\tau i}^k + F_{\tau,_z} N_i \boldsymbol{q}_{\tau i}^k \tag{18}$$

where $\boldsymbol{I} = \begin{bmatrix} 1 & 0 & 0 \\ 0 & 1 & 0 \\ 0 & 0 & 1 \end{bmatrix}$ and $F_{\tau,_z} = \dfrac{\partial F_\tau}{\partial z}$.

Upon substitution of Eqs. (17, 18) in Eq. (16), the internal virtual work takes the following form (subscripts τ and i are related to virtual variations, while subscript s and j concern the true quantities):

$$\begin{aligned}
&\int_{\Omega_k} \delta\boldsymbol{q}_{\tau i}^{kT}\boldsymbol{D}_p^T(N_i\boldsymbol{I})\tilde{\boldsymbol{C}}_{pp}^k\left[\int_{h_k}(F_\tau F_s)dz\right]\boldsymbol{D}_p(N_j\boldsymbol{I})\boldsymbol{q}_{sj}^k d\Omega_k \\
&+\int_{\Omega_k} \delta\boldsymbol{q}_{\tau i}^{kT}\boldsymbol{D}_p^T(N_i\boldsymbol{I})\tilde{\boldsymbol{C}}_{pn}^k\left[\int_{h_k}(F_\tau F_s)dz\right]\boldsymbol{D}_{n\Omega}(N_j\boldsymbol{I})\boldsymbol{q}_{sj}^k d\Omega_k \\
&+\int_{\Omega_k} \delta\boldsymbol{q}_{\tau i}^{kT}\boldsymbol{D}_p^T(N_i\boldsymbol{I})\tilde{\boldsymbol{C}}_{pn}^k\left[\int_{h_k}(F_\tau F_{s,_z})dz\right]N_j\boldsymbol{q}_{sj}^k d\Omega_k \\
&+\int_{\Omega_k} \delta\boldsymbol{q}_{\tau i}^{kT}\boldsymbol{D}_{n\Omega}^T(N_i\boldsymbol{I})\tilde{\boldsymbol{C}}_{np}^k\left[\int_{h_k}(F_\tau F_s)dz\right]\boldsymbol{D}_p(N_j\boldsymbol{I})\boldsymbol{q}_{sj}^k d\Omega_k \\
&+\int_{\Omega_k} \delta\boldsymbol{q}_{\tau i}^{kT}\boldsymbol{D}_{n\Omega}^T(N_i\boldsymbol{I})\tilde{\boldsymbol{C}}_{nn}^k\left[\int_{h_k}(F_\tau F_s)dz\right]\boldsymbol{D}_{n\Omega}(N_j\boldsymbol{I})\boldsymbol{q}_{sj}^k d\Omega_k \\
&+\int_{\Omega_k} \delta\boldsymbol{q}_{\tau i}^{kT}\boldsymbol{D}_{n\Omega}^T(N_i\boldsymbol{I})\tilde{\boldsymbol{C}}_{nn}^k\left[\int_{h_k}(F_\tau F_{s,_z})dz\right]N_j\boldsymbol{q}_{sj}^k d\Omega_k \\
&+\int_{\Omega_k} \delta\boldsymbol{q}_{\tau i}^{kT}N_i\tilde{\boldsymbol{C}}_{np}^k\left[\int_{h_k}(F_{\tau,_s} F_s)dz\right]\boldsymbol{D}_p(N_j\boldsymbol{I})\boldsymbol{q}_{sj}^k d\Omega_k \\
&+\int_{\Omega_k} \delta\boldsymbol{q}_{\tau i}^{kT}N_i\tilde{\boldsymbol{C}}_{nn}^k\left[\int_{h_k}(F_{\tau,_z} F_s)dz\right]\boldsymbol{D}_{n\Omega}(N_j\boldsymbol{I})\boldsymbol{q}_{sj}^k d\Omega_k \\
&+\int_{\Omega_k} \delta\boldsymbol{q}_{\tau i}^{kT}N_i\tilde{\boldsymbol{C}}_{nn}^k\left[\int_{h_k}(F_{\tau,_s} F_{s,_z})dz\right]N_j\boldsymbol{q}_{sj}^k d\Omega_k = \delta L_i^k.
\end{aligned} \tag{19}$$

As usual in two-dimensional modelings, the integration through the thickness-direction can be made a priori. The following layer-integrals are introduced:

$$\begin{aligned}
&(E_{\tau s},\, E_{\tau s,_z},\, E_{\tau,_z s},\, E_{\tau,_z s,_z}) \\
&\quad = \int_{h_k} (F_\tau F_s,\, F_\tau F_{s,_z},\, F_{\tau,_z} F_s,\, F_{\tau,_z} F_{s,_z}) dz.
\end{aligned} \tag{20}$$

If the following laminate stiffness definitions are considered:

$$\left(\tilde{\boldsymbol{Z}}_{pp}^{k\tau s},\, \tilde{\boldsymbol{Z}}_{pn}^{k\tau s},\, \tilde{\boldsymbol{Z}}_{np}^{k\tau s},\, \tilde{\boldsymbol{Z}}_{nn}^{k\tau s}\right) = \left(\tilde{\boldsymbol{C}}_{pp}^k,\, \tilde{\boldsymbol{C}}_{pn}^k,\, \tilde{\boldsymbol{C}}_{np}^k,\, \tilde{\boldsymbol{C}}_{nn}^k\right) E_{\tau s}; \tag{21}$$

$$\begin{aligned}
&\left(\tilde{\boldsymbol{Z}}_{pn}^{k\tau s,_z},\, \tilde{\boldsymbol{Z}}_{nn}^{k\tau s,_z},\, \tilde{\boldsymbol{Z}}_{np}^{k\tau,_z s},\, \tilde{\boldsymbol{Z}}_{nn}^{k\tau,_z s},\, \tilde{\boldsymbol{Z}}_{nn}^{k\tau,_z s,_z}\right) \\
&\quad = \left(\tilde{\boldsymbol{C}}_{pn}^k E_{\tau s,_z},\, \tilde{\boldsymbol{C}}_{nn}^k E_{\tau,s,_z},\, \tilde{\boldsymbol{C}}_{np}^k E_{\tau,_z s},\, \tilde{\boldsymbol{C}}_{nn}^k E_{\tau,_z s}^k,\, \tilde{\boldsymbol{C}}_{nn}^k E_{\tau,_z s,_z}\right),
\end{aligned} \tag{22}$$

Eq. (19) can be written in the compact form:

$$\delta\mathbf{q}_{\tau i}^{kT}\mathbf{K}^{k\tau sij}\mathbf{q}_{sj}^k = \delta L_i^k, \tag{23}$$

where the explicit form of $\mathbf{K}^{k\tau sij}$ is:

$$\begin{aligned}
\boldsymbol{K}^{k\tau sij} &= \triangleleft \boldsymbol{D}_p^T(N_i\boldsymbol{I})\left[\tilde{\boldsymbol{Z}}_{pp}^{k\tau s}\boldsymbol{D}_p(N_j\boldsymbol{I}) + \tilde{\boldsymbol{Z}}_{pn}^{k\tau s} \times \boldsymbol{D}_{n\Omega}(N_j\boldsymbol{I}) + \tilde{\boldsymbol{Z}}_{pn}^{k\tau s,_z}N_j\right] \\
&+ \boldsymbol{D}_{n\Omega}^T(N_i\boldsymbol{I})\left[\tilde{\boldsymbol{Z}}_{np}^{k\tau s}\boldsymbol{D}_p(N_j\boldsymbol{I}) + \tilde{\boldsymbol{Z}}_{nn}^{k\tau s}\boldsymbol{D}_{n\Omega}(N_j\boldsymbol{I}) + \tilde{\boldsymbol{Z}}_{nn}^{k\tau s,_z}N_j\right] \\
&+ N_i\left[\tilde{\boldsymbol{Z}}_{np}^{k\tau,_z s}\boldsymbol{D}_p(N_j\boldsymbol{I}) + \tilde{\boldsymbol{Z}}_{nn}^{k\tau,_z s}\boldsymbol{D}_{n\Omega}(N_j\boldsymbol{I}) + \tilde{\boldsymbol{Z}}_{nn}^{k\tau,_z s,_z}\cdot N_j\right]\triangleright_\Omega.
\end{aligned} \tag{24}$$

The symbol $\triangleleft \ldots \triangleright_\Omega$ denotes the integral on Ω. The matrix $\mathbf{K}^{k\tau sij}$ is a 3×3 array and it consists of the stiffness matrix fundamental nucleus: it contains all the information to built the stiffness matrix. The explicit form of $\boldsymbol{K}^{k\tau sij}$ is listed below:

$$\begin{aligned}
K_{11}^{k\tau sij} &= \tilde{Z}_{pp11}^{k\tau s}\triangleleft N_{i,x}N_{j,x}\triangleright_\Omega + \tilde{Z}_{pp16}^{k\tau s}\triangleleft N_{i,y}N_{j,x}\triangleright_\Omega + \tilde{Z}_{pp16}^{k\tau s}\triangleleft \\
&\quad N_{i,x}N_{j,y}\triangleright_\Omega + \tilde{Z}_{pp66}^{k\tau s}\triangleleft N_{i,y}N_{j,y}\triangleright_\Omega + \tilde{Z}_{pp55}^{k\tau,_z s,_z}\triangleleft N_i N_j\triangleright_\Omega
\end{aligned}$$

$$K_{12}^{k\tau sij} = \tilde{Z}_{pp12}^{k\tau s} \lhd N_{i,x} N_{j,y} \rhd_\Omega + \tilde{Z}_{pp26}^{k\tau s} \lhd N_{i,y} N_{j,y} \rhd_\Omega + \tilde{Z}_{pp16}^{k\tau s} \lhd N_{i,x} N_{j,x} \rhd_\Omega + \tilde{Z}_{pp66}^{k\tau s} \lhd N_{i,y} N_{j,x} \rhd_\Omega + \tilde{Z}_{pp45}^{k\tau,_z s,_z} \lhd N_i N_j \rhd_\Omega$$

$$K_{13}^{k\tau sij} = \tilde{Z}_{pn13}^{k\tau s,_z} \lhd N_{i,x} N_j \rhd_\Omega + \tilde{Z}_{pn36}^{k\tau s,_z} \lhd N_{i,y} N_j \rhd_\Omega + \tilde{Z}_{nn55}^{k\tau,_z s} \lhd N_i N_{j,x} \rhd_\Omega + \tilde{Z}_{nn45}^{k\tau,_z s} \lhd N_i N_{j,y} \rhd_\Omega$$

$$K_{21}^{k\tau sij} = \tilde{Z}_{pp12}^{k\tau s} \lhd N_{i,y} N_{j,x} \rhd_\Omega + \tilde{Z}_{pp16}^{k\tau s} \lhd N_{i,x} N_{j,x} \rhd_\Omega + \tilde{Z}_{pp26}^{k\tau s} \lhd N_{i,y} N_{j,y} \rhd_\Omega + \tilde{Z}_{pp66}^{k\tau s} \lhd N_{i,x} N_{j,y} \rhd_\Omega + \tilde{Z}_{nn45}^{k\tau,_z s,_z} \lhd N_i N_j \rhd_\Omega$$

$$K_{22}^{k\tau sij} = \tilde{Z}_{pp22}^{k\tau s} \lhd N_{i,y} N_{j,y} \rhd_\Omega + \tilde{Z}_{pp26}^{k\tau s} \lhd N_{i,x} N_{j,y} \rhd_\Omega + \tilde{Z}_{pp26}^{k\tau s} \lhd N_{i,y} N_{j,x} \rhd_\Omega + \tilde{Z}_{pp66}^{k\tau s} \lhd N_{i,x} N_{j,x} \rhd_\Omega + \tilde{Z}_{nn44}^{k\tau,_z s,_z} \lhd N_i N_j \rhd_\Omega$$

$$K_{23}^{k\tau sij} = \tilde{Z}_{pn23}^{k\tau s,_z} \lhd N_{i,y} N_j \rhd_\Omega + \tilde{Z}_{pn36}^{k\tau s,_z} \lhd N_{i,x} N_j \rhd_\Omega + \tilde{Z}_{nn45}^{k\tau,_z s} \lhd N_i N_{j,x} \rhd_\Omega + \tilde{Z}_{nn44}^{k\tau,_z s} \lhd N_i N_{j,y} \rhd_\Omega$$

$$K_{31}^{k\tau sij} = \tilde{Z}_{nn55}^{k\tau s,_z k} \lhd N_{i,x} N_j \rhd_\Omega + \tilde{Z}_{nn45}^{k\tau s,_z k} \lhd N_{i,y} N_j \rhd_\Omega + \tilde{Z}_{pp13}^{k\tau,_z s} \lhd N_i N_{j,x} \rhd_\Omega + \tilde{Z}_{pp36}^{k\tau,_z s} \lhd N_i N_{j,y} \rhd_\Omega$$

$$K_{32}^{k\tau sij} = \tilde{Z}_{nn45}^{k\tau s,_z k} \lhd N_{i,x} N_j \rhd_\Omega + \tilde{Z}_{nn44}^{k\tau s,_z k} \lhd N_{i,y} N_j \rhd_\Omega + \tilde{Z}_{np23}^{k\tau,_z s} \lhd N_i N_{j,y} \rhd_\Omega + \tilde{Z}_{np36}^{k\tau,_z s} \lhd N_i N_{j,x} \rhd_\Omega$$

$$K_{33}^{k\tau sij} = \tilde{Z}_{nn55}^{k\tau sk} \lhd N_{i,x} N_{j,x} \rhd_\Omega + \tilde{Z}_{nn45}^{k\tau sk} \lhd N_{i,y} N_{j,x} \rhd_\Omega + \tilde{Z}_{nn45}^{k\tau sk} \lhd N_{i,x} N_{j,y} \rhd_\Omega + \tilde{Z}_{nn44}^{k\tau sk} \lhd N_{i,y} N_{j,y} \rhd_\Omega + \tilde{Z}_{nn33}^{k\tau,_z s,_z} \lhd N_i N_j \rhd_\Omega. \quad (25)$$

The external work of applied loadings and the inertial work can be written in terms of nodal quantities, according to the expansion in Eq. (2) and to the discretization in (12). The external load becomes:

$$\delta L_e^k = \delta \boldsymbol{q}_{\tau i}^{kT} \boldsymbol{P}_{\tau i}^k \quad (26)$$

The inertial load leads to the fundamental nucleus of the inertial matrix $\boldsymbol{M}^{\tau sij}$, which is a 3×3 array. Non-zero elements of $\boldsymbol{M}^{\tau sij}$ are:

$$M_{11}^{k\tau sij} = M_{22}^{k\tau sij} = M_{33}^{k\tau sij} \rho^k \lhd N_i N_j \rhd_{\Omega_k} F_\tau F_s.$$

Whatever is the variables' description, starting from the corresponding fundamental nuclei, for a given thickness expansion and discretization the mass matrix $\boldsymbol{M}$ and the stiffness matrix $\boldsymbol{K}$ can be calculated by numerical integration and the assembly procedure. In case of ESL theory, the number of obtained equations coincides with the number of introduced variables: τ and s vary from 0 to N, i and j vary from 1 to N_n and k ranges from 1 to N_l. If LW theory is addressed to, after the assembly procedure, the number of equations able to model the multilayered structure is higher with respect to the case of ESL of factor $\frac{1}{2}(N_l + 1)$.

4.3. Static Problem

If the static problem is considered, the internal work must be equal to the external work. That is:

$$\delta \boldsymbol{q}_{\tau i}^{kT} \boldsymbol{K}^{k\tau sij} \boldsymbol{q}_{sj}^k = \delta \boldsymbol{q}_{\tau i}^{kT} \boldsymbol{P}_{sj}^k. \quad (27)$$

By imposing the definition of virtual variations, the following equilibrium conditions is obtained:

$$\delta \boldsymbol{q}_{\tau i}^{kT} : \quad \boldsymbol{K}^{k\tau sij} \boldsymbol{q}_{sj}^k = \boldsymbol{P}_{sj}^k. \quad (28)$$

In order to write the stiffness matrix for the whole multilayered plate, the couples of index (τ, s) and (i, j) in the stiffness fundamental nucleus $\boldsymbol{K}^{k\tau sij}$ have to be expanded. Further details of the assembly procedure can be read in [27].

The final system to be solved is the following:

$$\boldsymbol{K}\boldsymbol{q} = \boldsymbol{P}, \quad (29)$$

where $\boldsymbol{q}$ is the vector of nodal unknowns and $\boldsymbol{P}$ is the vector of nodal loads.

4.4. Dynamic Problem

If the dynamic problem is considered, the inertial contribution must be included in the formulation. Eq. (27) becomes:

$$\delta \boldsymbol{q}_{\tau i}^{kT} \boldsymbol{M}^{k\tau sij} \ddot{\boldsymbol{q}}_{sj}^k + \delta \boldsymbol{q}_{\tau i}^{kT} \boldsymbol{K}^{k\tau sij} \boldsymbol{q}_{sj}^k = \delta \boldsymbol{q}_{\tau i}^{kT} \boldsymbol{P}_{sj}^k, \quad (30)$$

and Eq. (28) becomes:

$$\delta \boldsymbol{q}_{\tau i}^{k} : \quad \boldsymbol{M}^{k\tau sij} \ddot{\boldsymbol{q}}_{sj}^k + \boldsymbol{K}^{k\tau sij} \boldsymbol{q}_{sj}^k = \boldsymbol{P}_{sj}^k. \quad (31)$$

The undamped dynamic problem can be written in terms of the following ordinary differential equations system:

$$\boldsymbol{M}\ddot{\boldsymbol{q}} + \boldsymbol{K}_q = \boldsymbol{P}, \quad (32)$$

In case of free vibration analysis, the i-th natural frequency ω_i can be calculated by solving the generalized eigenvalues problem:

$$(-\omega_i^2 \boldsymbol{M} + \boldsymbol{K})\boldsymbol{a}_i = \boldsymbol{0}, \quad (33)$$

where $\boldsymbol{a}_i$ is the i-th eigenvector.

4.5. Acronyms

Depending on the kinematic assumptions, on the order of expansion and on the choice of the thickness functions, different acronyms are here introduced in order to distinguish the corresponding FEs. Fig. 2 shows how the acronyms are built: the first field can be "E" or "L", according to the ESL or LW kinematic description, respectively; the second field "D" means that the PVD variational statement is applied (only PVD applications are presented in this paper); the third field can assume the numbers 1–4, according to the order of the adopted expansion in the plate-thickness direction; the last field identifies the polynomial choice for the thickness expansion.

Downloaded By: [Nali, Pietro] At: 11:45 8 November 2010

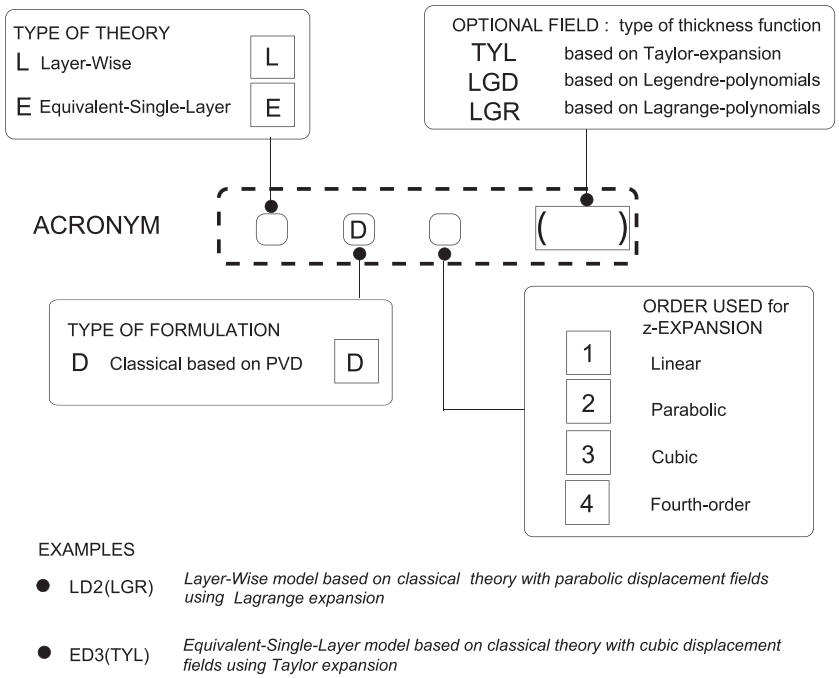

FIG. 2. Used FEs acronyms.

TABLE 2
Convergency for $\tilde{u}_3$ and $\tilde{\sigma}_{11}$ in the center of the plate - Problem I

$\tilde{u}_3$		top	middle	bottom
	3D Pagano	7.738	7.391	7.269
10×1	ED3(TYL)	7.190	6.836	6.707
	ED3(LGR)	6.818	6.484	6.346
	ED3(LGD)	6.818	6.484	6.346
30×1	ED3(TYL)	7.229	6.876	6.747
	ED3(LGR)	6.859	6.526	6.389
	ED3(LGD)	6.859	6.526	6.389
50×1	ED3(TYL)	7.232	6.880	6.751
	ED3(LGR)	6.863	6.530	6.392
	ED3(LGD)	6.863	6.530	6.392
$\tilde{\sigma}_{11}$		top	middle	bottom
	3D Pagano	18.81	0.09762	−18.10
10×1	ED3(TYL)	17.99	0.10594	−17.26
	ED3(LGR)	19.74	0.10917	−18.96
	ED3(LGD)	19.74	0.10917	−18.96
30×1	ED3(TYL)	18.16	0.10404	−17.43
	ED3(LGR)	19.95	0.10731	−19.18
	ED3(LGD)	19.95	0.10731	−19.18
50×1	ED3(TYL)	18.17	0.10389	−17.44
	ED3(LGR)	19.97	0.10716	−19.20
	ED3(LGD)	19.97	0.10716	−19.20

5. NUMERIC RESULTS AND DISCUSSION

Four different plate problems whose details are given below are considered in the following.

Problem I Pagano cylindrical bending: the structure is a symmetric 3-ply laminate with stacking se-quence 0°/90°/0°. Layers are of same material and of equal equal thickness $a/h = 4$. Material properties are:

$E_L = 25 \times 10^6$ psi, $E_T = 10^6$ psi, $G_{LT} = 0.5 \times 10^6$ psi, $G_{TT} = 0.2 \times 10^6$ psi, $v_{LT} = v_{TT} = 0.25$.

TABLE 3
$\tilde{u}_3$ in the center of the plate with 50×1 mesh - Problem I

$\tilde{u}_3$	top	middle	bottom
3D Pagano	7.738	7.391	7.269
ED1(TYL)	5.591	5.360	5.129
ED2(TYL)	5.630	5.311	5.149
ED3(TYL)	7.232	6.880	6.751
ED4(TYL)	7.237	6.879	6.755
EDl(LGR)	6.137	5.905	5.673
ED2(LGR)	6.164	5.852	5.694
ED3(LGR)	6.863	6.530	6.392
ED4(LGR)	6.869	6.528	6.398
EDl(LGD)	6.137	5.905	5.673
ED2(LGD)	6.164	5.852	5.694
ED3(LGD)	6.863	6.530	6.392
ED4(LGD)	6.869	6.528	6.398

Downloaded By: [Nali, Pietro] At: 11:45 8 November 2010

The laminate is simply supported at the tips $x = 0$ and $x = a$. Following sinusoidal pressure $p = p_0 \sin(\pi x/a)$ is applied at the top of the plate.

Results for the displacements u_1, u_3 and for stresses σ_{11}, σ_{13} and σ_{33} are presented in dimensionless form according to:

$$\tilde{u}_1 = \frac{E_T u_1(0,z)}{h p_0} \quad \tilde{u}_3 = \frac{E_T u_3(\alpha/2,z)}{h p_0},$$
$$\tilde{\sigma}_{11} = \frac{\sigma_{11}(\alpha/2,z)}{p_0}, \quad \tilde{\sigma}_{33} = \frac{\sigma_{33}(\alpha/2,z)}{p_0}, \quad \tilde{\sigma}_{13} = \frac{\sigma_{13}(0,z)}{p_0},$$

where dimensionless quantities are indicated with the tilde symbol "∼".

Problem II Four-edge simply supported single layer square plate made of isotropic material: $a = b = 0.5$ m, $a/h = 250$, $E = 73$ GPa, $\upsilon = 0.34$, $\rho = 2800$ kg/m^3 - undamped free vibrations analysis.

Problem III Fully clamped single layer square plate made of orthotropic material: $a = b = 0.3$ m, $a/h = 93.75$, $E_1 = 14.17$ GPa, $E_2 = E_3 = 8.88$ GPa, $G_{12} = G_{13} = G_{23} = 2.93$ GPa, $\upsilon_{12} = \upsilon_{13} = \upsilon_{23} = 0.295$; $\rho = 1771.5$ kg/m^3- undamped free vibrations analysis.

Problem IV Four-edge simply supported multilayered orthotropic square plate with cross-ply non sym-metric (0°/90°) and symmetric (0°/90°/0°) stacking sequence (layer thickness is the same for 90° and 0° oriented laminae): $a/h = 5$, $G_{LT}/E_T = G_{LZ}/E_T = 0.50$, $G_{TT}/E_T = 0.35$, $\upsilon_{LT} = \upsilon_{LZ} = 0.3$, $\upsilon_{TT} = 0.49$. Three E_L/E_T ratios are considered. L signifies the fiber direction and T the transverse direction - undamped free vibrations analysis.

TABLE 4
Undamped natural frequencies $\omega_{(m,n)}$ with m, n = number of half-waves in the plane x and y directions. (*) The free vibration frequencies are computed on the basis of homogeneous isotropic thin plate theory - Problem II

frequency modes $\omega_{(m,n)}$	(1, 1)	(2, 1)	(1, 2)	(2, 2)
Analytical values* [31]				
	39.7	98.2	98.2	157.2
Q4, 8 × 8				
EDl(TYL)	40.1	104.9	104.9	168.9
EDl(LGR)	40.1	104.9	104.9	168.9
EDI (LGD)	40.1	104.9	104.9	168.9
Q4, 10 × 10				
EDl(TYL)	39.8	102.5	102.5	164.7
EDl(LGR)	39.8	102.5	102.5	164.7
EDI (LGD)	39.8	102.5	102.5	164.7
Q4 12 × 12				
EDl(TYL)	39.7	101.3	101.3	162.4
EDl(LGR)	39.7	101.3	101.3	162.4
EDI (LGD)	39.7	101.3	101.3	162.4

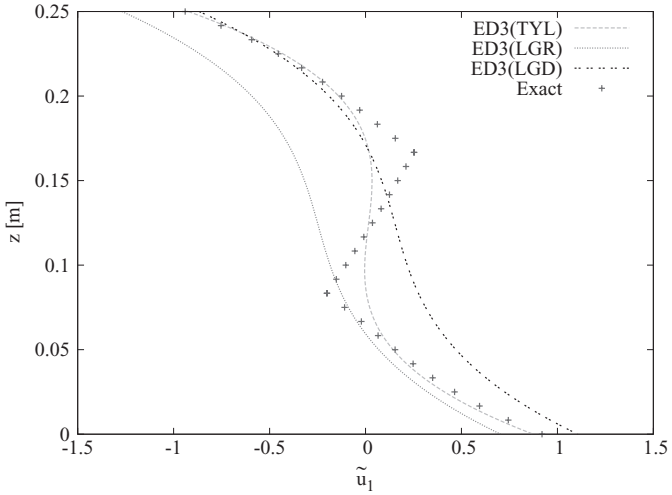

FIG. 3. Comparison 3-rd order ED results obtained with different polynomial expansion: quantity $\tilde{u}_1$- Problem I.

FEM results showed in this paper are obtained by MUL2 software. MUL2 is an academic software implemented according to the formulation here proposed.

5.1. Equivalent Single Layer

The three polynomial choices (Taylor, Legendre and Lagrange) are first considered for the thickness ex-pansion in the framework of ESL modeling of plates. It should be noted that no results are available in literature in which Legendre and Lagrange polynomials are employed with ESL kinematics.

5.1.1. Cylindrical Bending

Convergence analysis for the cylindrical bending in Problem I proposed by Pagano [28] is first considered in Tabs. 2, 3. The accuracy level of various meshes of Q4 FEs is investigated (Q4

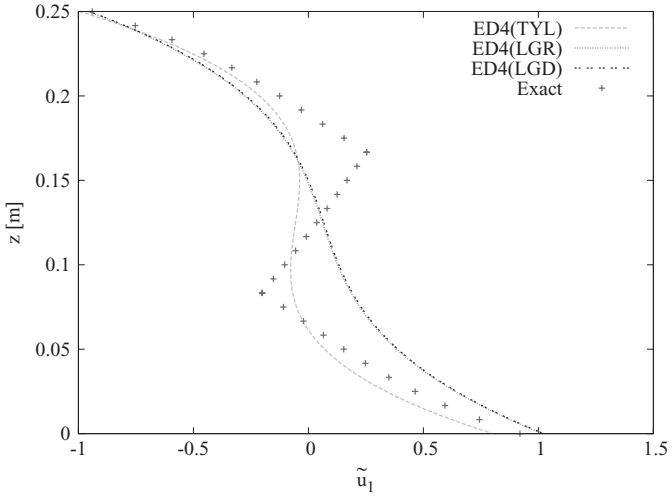

FIG. 4. Comparison 4-th order ED results obtained with different polynomial expansion: quantity $\tilde{u}_1$- Problem I.

Downloaded By: [Nali, Pietro] At: 11:45 8 November 2010

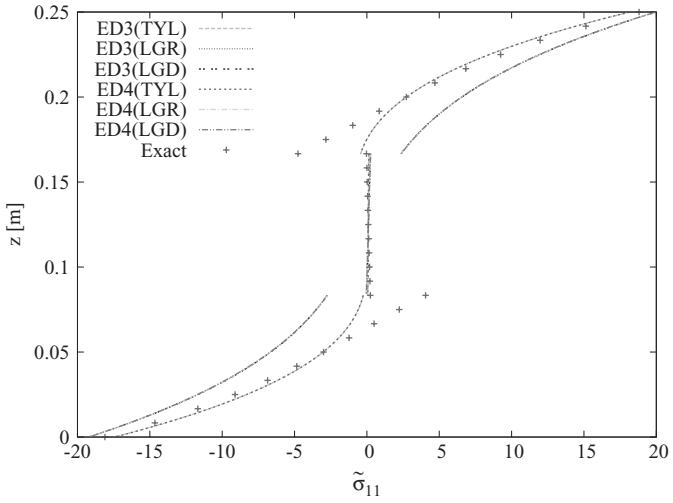

FIG. 5. Comparison ED results obtained with different polynomial expansion: quantity $\tilde{\sigma}_{11}$- Problem I.

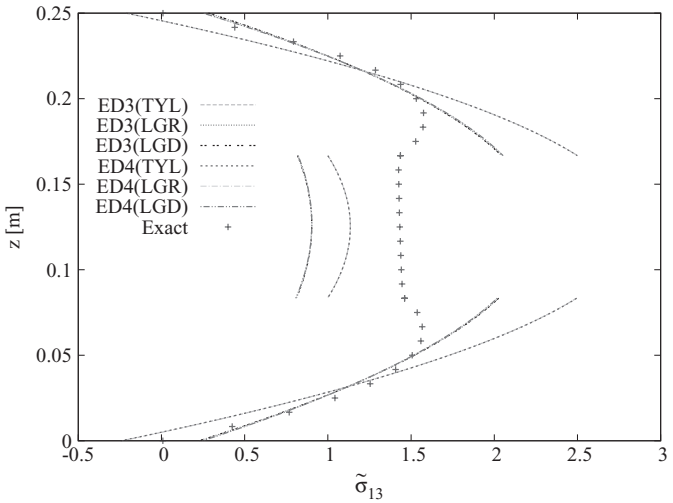

FIG. 7. Comparison ED results obtained with different polynomial expansion: quantity $\tilde{\sigma}_{13}$- Problem I.

Downloaded By: [Nali, Pietro] At: 11:45 8 November 2010

denotes the 4-node Quadrangular finite elements). The mesh refinement starts from 10×1 and ranges until 50×1. Transverse displacement and in-plane stress values at the plate top, middle and bottom positions are compared with Pagano's corresponding 3D exact solution [28]. The present results were first assessed with closed form solutions [29]. This assessment is here omitted for the sake of brevity. The results are restricted to third order thickness expansion, however the results related to lower ($N = 1, 2$) and higher ($N = 4$) orders of expansion, which are here omitted for sake of brevity, behave in the same way as the case of $N = 3$. The differences from the 3D solution are mostly experienced in thick plate geometries. The convergence rate does not depend on the polynomial choice and is the typical one of serendipity plate elements [30]. Various order-N values are compared in Tab. 3. In-plane displacement values are

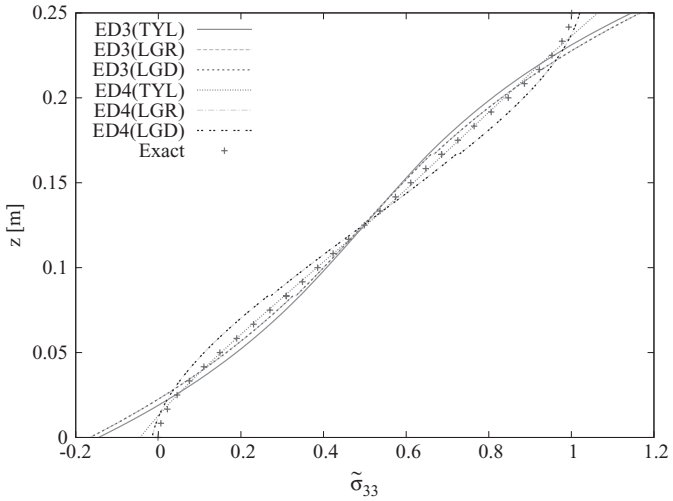

FIG. 6. Comparison ED results obtained with different polynomial expansion: quantity $\tilde{\sigma}_{33}$- Problem I.

considered. Better accuracy is obtained by increasing the order in the three cases. Different approaches lead to different distributions of the variables through the thickness of the plate. This justifies the fact that a single-point comparison between results obtained with various approaches is not sufficient to asses the corresponding level of accuracy. A more complete picture can be obtained by looking at the distribution of the stresses and displacement variables through the thickness-plate direction. This is shown in Figs. 3–7. It appears clear that the error related to the different polynomials assumptions depends to a great extent on the z-position. General conclusions on the fairness of a given approach cannot be made.

5.1.2. Undamped Free Vibrations Analysis

Free vibration results are given in Tabs. 4–7, where comparisons between FEM analyses and closed-form solutions are given. First order through-the-thickness assumptions are considered both in the FE analysis and in the analytical solutions. Higher order modelings are only considered in Tab. 7, in which the 3D solution is given.

Plate Problem II is considered in Tab. 4. The first four undamped free vibration frequencies are given for three different FE meshes: the good convergence rate experienced in bending problems is confirmed.

As for the multilayered plate of problem III, the first seven frequencies are compared in Tabs. 5, 6, where FEM results are obtained with Q4 and Q9 FEs, respectively. It should be remarked that the Q9 FEs are not of the serendipity-type. It has been confirmed that neither the accuracy nor the convergence rate significantly affected by the polynomial choice.

The effect of the orthotropic ratio as well as of the number of layers is considered in Tab. 7 for the cross-ply plates of Problem IV. The accuracy of higher order models is more evident in the case of non-symmetrically laminated plates as well as in the case of higher orthotropic ratio values.

TABLE 5

Convergency study for the first 7 undamped natural frequencies ω_i with Q4 element; (*) The free vibration frequencies are computed on the basis of homogeneous orthotropic and anisotropic thin plate theory. Approximate closed-form expressions is referred to, see [32] - Problem III

frequency number ω_i	1	2	3	4	5	6	7
Analytical values*							
	150.39	284.49	330.18	444.91	502.75	610.52	646.42
Q4, 8×8							
EDl(TYL)	155.42	313.62	367.92	493.60	635.72	779.95	781.21
EDl(LGR)	155.42	313.62	367.92	493.60	635.72	779.95	781.21
EDl(LGD)	155.42	313.62	367.92	493.60	635.72	779.95	781.21
Q4, 12×12							
EDl(TYL)	151.70	294.59	343.52	461.26	550.08	670.97	692.85
EDl(LGR)	151.70	294.59	343.52	461.26	550.08	670.97	692.85
EDl(LGD)	151.70	294.59	343.52	461.26	550.08	670.97	692.85
Q4, 16×16							
EDl(TYL)	150.45	288.52	335.74	450.88	525.27	639.34	666.70
EDl(LGR)	150.45	288.52	335.74	450.88	525.27	639.34	666.70
EDl(LGD)	150.45	288.52	335.74	450.88	525.27	639.34	666.70

Downloaded By: [Nali, Pietro] At: 11:45 8 November 2010

5.2. Comparison of Various Thickness Expansions in the Case of the LW Theory

5.2.1. Cylindrical Bending

Most of the problems considered in the ESL case are hereafter extended to the LW approach. LW imple-mentation is restricted to Legendre and Lagrange polynomials. In fact, the use of a Taylor-type expansion would require additional constraint equations (written by means of Lagrange multipliers) to impose the continuity of displacements at the interfaces between the layers.

A good convergence rate has been confirmed for the cylindrical bending in problem I; the results are quoted in Tab. 8. Additional results are given in Tabs. 9, 10 as well as in Figs. 8–14: a quite exhaustive comparison between LW models based on Legendre and Lagrange polynomials is given for the case of linear up-to-fourth order expansion; through-the-thickness

TABLE 6

Convergency study for the first 7 undamped natural frequencies ω_i with Q9 element; (*) The free vibration frequencies are computed on the basis of homogeneous orthotropic and anisotropic thin plate theory. Approximate closed-form expressions is referred to, see [32] - Problem III

frequency number ω_i	1	2	3	4	5	6	7
Analytical values*							
	150.39	284.49	330.18	444.91	502.75	610.52	646.42
Q9, 3×3							
EDl(TYL)	150.43	303.21	355.17	479.04	616.02	752.31	756.65
EDl(LGR)	150.43	303.21	355.17	479.04	616.02	752.31	756.65
EDl(LGD)	150.43	303.21	355.17	479.04	616.02	752.31	756.65
Q9, 6×6							
EDl(TYL)	148.96	282.29	327.84	440.30	505.81	614.60	645.08
EDl(LGR)	148.96	282.29	327.84	440.30	505.81	614.60	645.08
EDl(LGD)	148.96	282.29	327.84	440.30	505.81	614.60	645.08
Q9, 9×9							
EDl(TYL)	148.89	281.34	326.57	438.59	498.33	604.98	637.73
EDl(LGR)	148.89	281.34	326.57	438.59	498.33	604.98	637.73
EDl(LGD)	148.89	281.34	326.57	438.59	498.33	604.98	637.73

Downloaded By: [Nali, Pietro] At: 11:45 8 November 2010

TABLE 7
Undamped natural frequencies in dimensionless form: $\tilde{\omega} = \omega h\sqrt{\rho/E_T}$-Problem IV

N_l E_L/E_T		2		3
		3	30	3
Analytical values [29]				
		0.2392	0.3117	0.2516
ED4		0.2394	0.3133	0.2518
ED3		0.2394	0.3167	0.2519
ED2		0.2418	0.3198	0.2569
EDI		0.2662	0.3367	0.2778
Q9, 3×3				
ED4(TYL)		0.2398	0.3138	0.2523
ED3(TYL)		0.2399	0.3172	0.2523
ED2(TYL)		0.2423	0.3203	0.2573
EDl(TYL)		0.2459	0.3272	0.2587
ED4(LGR)		0.2551	0.4141	0.2551
ED3(LGR)		0.2551	0.4143	0.2551
ED2(LGR)		0.2587	0.4335	0.2587
EDl(LGR)		0.2640	0.4343	0.2640
ED4(LGD)		0.2551	0.4141	0.2551
ED3(LGD)		0.2551	0.4143	0.2551
ED2(LGD)		0.2587	0.4335	0.2587
EDl(LGD)		0.2640	0.4343	0.2640
Q9, 6×6				
ED3(TYL)		0.2395	0.3168	0.2519
ED3(LGR)		0.2547	0.4139	0.2547
ED3 (LCD)		0.2547	0.4139	0.2547

distributions of displacement components and of transverse and shear stress variables are considered. Appropriate LW analysis lead to three-dimensional descriptions of the displacement and stress states. Almost the same accuracy is obtained with Legendre and Lagrange expansions for a fixed order. It should

TABLE 8
Convergency for $\tilde{u}_3$ and $\tilde{\sigma}_{11}$ in the center of the plate - Problem I

u_3		top	middle	bottom
	3D Pagano	7.738	7.391	7.269
10×1	LD3(LGD)	7.795	7.426	7.303
30×1	LD3(LGD)	7.763	7.399	7.278
50×1	LD3(LGD)	7.760	7.397	7.276
σ_{11}		top	middle	bottom
	3D Pagano	18.81	0.09762	−18.10
10×1	LD3(LGD)	18.62	0.09904	−17.90
30×1	LD3(LGD)	18.79	0.09723	−18.08
50×1	LD3(LGD)	18.80	0.09708	−18.09

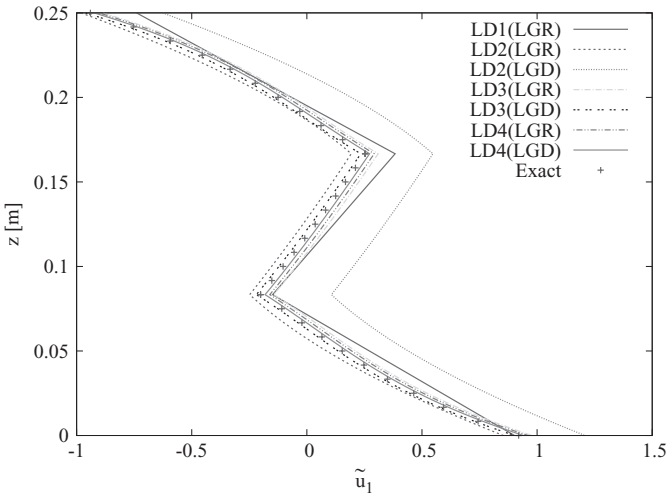

FIG. 8. Comparison LDn(LGR/LGD) results obtained with different polynomial order: quantity $\tilde{u}_1$- Problem I.

be underlined that such accuracy is mostly subordinate to the z-position along the plate thickness direction.

5.2.2. Undamped Free Vibrations Analysis

The same conclusions given in Sec. 5.2.1 have been confirmed for free undamped vibrations, see Tabs. 11, 12. The capability of the LW approach to reach SD-results is here confirmed.

5.3. FE models Accuracy vs nDOFs

Different polynomials choices and various orders of expansion for the thickness functions are provided in this section for further comparisons between ESL and LW theories. The aim is to try to provide an answer to the question: what is the most reliable and computational efficient FE model?

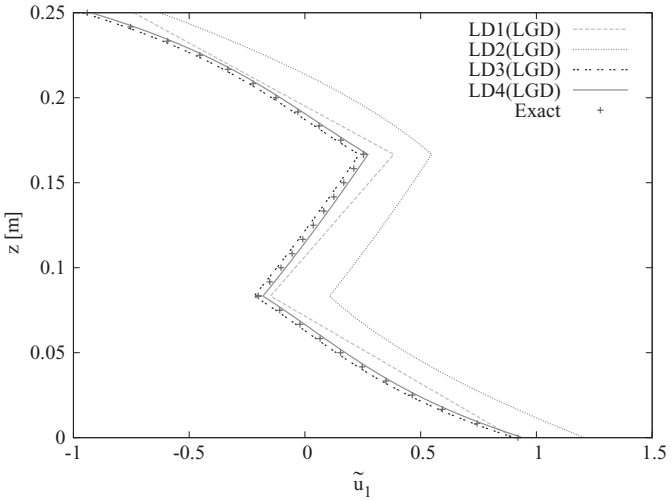

FIG. 9. Comparison LDn(LGD) results obtained with different polynomial order: quantity $\tilde{u}_1$-Problem I.

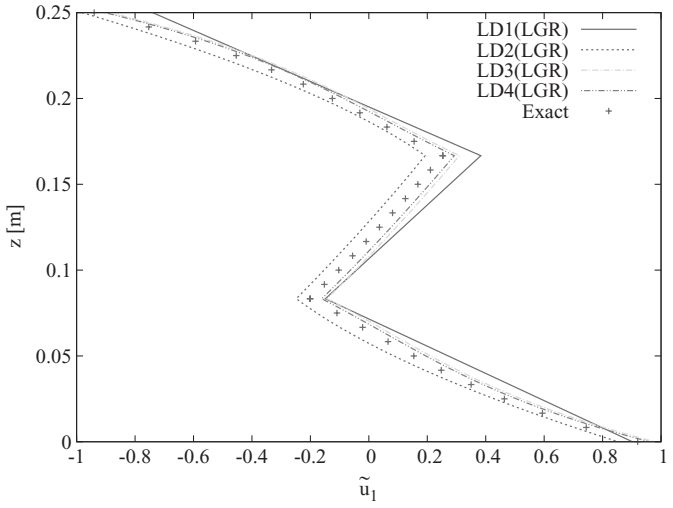

FIG. 10. Comparison LDn(LGR) results obtained with different polynomial order: quantity $\tilde{u}_1$-Problem I.

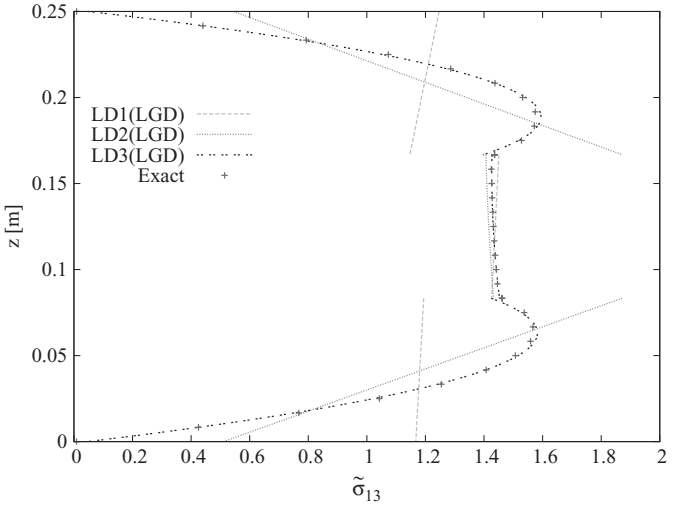

FIG. 13. Comparison LDn(LGD) results obtained with different polynomial order: quantity $\tilde{\sigma}_{13}$-Problem I.

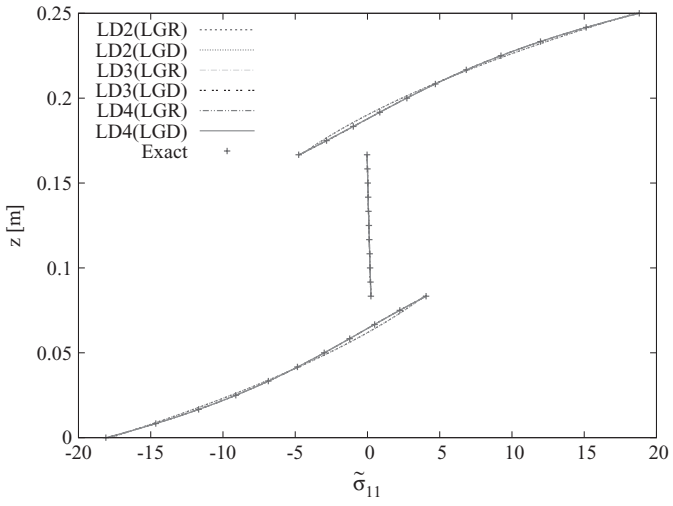

FIG. 11. Comparison LDn(LGR/LGD) results obtained with different polynomial order: quantity $\tilde{\sigma}_{11}$-Problem I.

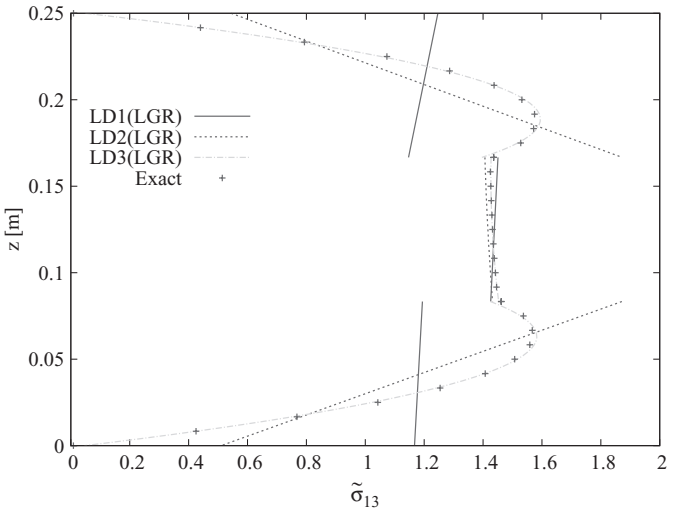

FIG. 14. Comparison LDn(LGR) results obtained with different polynomial order: quantity $\tilde{\sigma}_{13}$-Problem I.

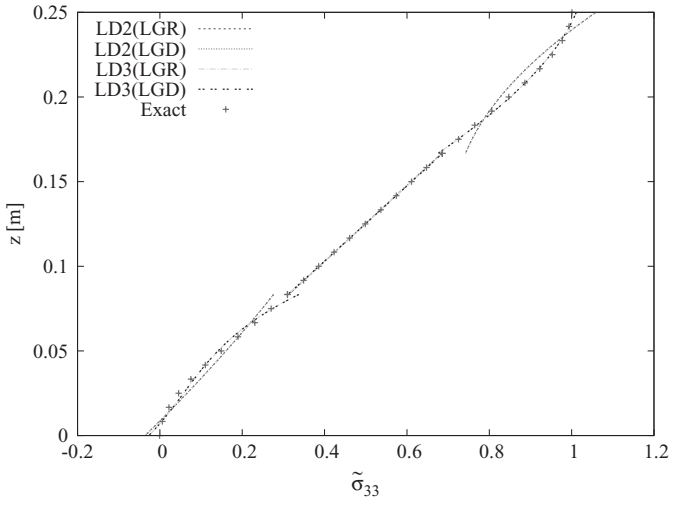

FIG. 12. Comparison LDn(LGR/LGD) results obtained with different polynomial order: quantity $\tilde{\sigma}_{33}$-Problem I.

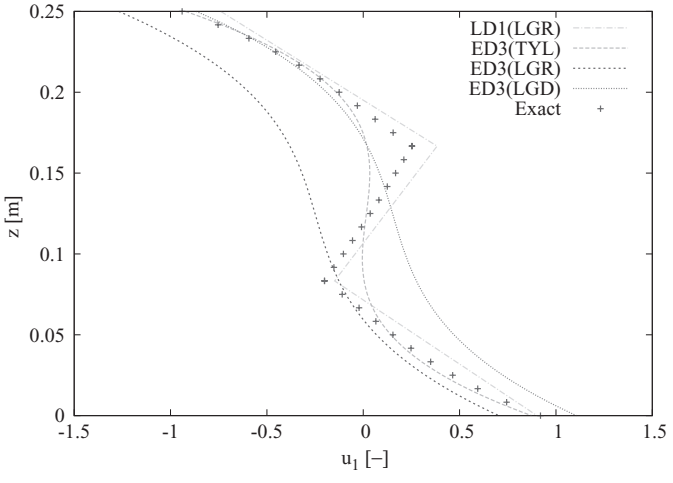

FIG. 15. Comparison between ED3 and LD1 theories with the same nDOFs: $\tilde{u}_1$-quantity-Problem I.

Downloaded By: [Nali, Pietro] At: 11:45 8 November 2010

Downloaded By: [Nali, Pietro] At: 11:45 8 November 2010

TABLE 9
$\tilde{u}_1$ in the edge of the plate with 50 × 1 mesh - Problem I

	top	middle	bottom
3D Pagano	−0.940	0.0364	0.920
LD1 (LGR)	−0.740	0.117	0.902
LD2 (LGR)	−0.981	−0.0171	0.854
LD3 (LGR)	−0.885	−0.0937	0.979
LD4 (LGR)	−0.903	0.0762	0.962
LD1 (LGD)	−0.740	0.117	0.902
LD2 (LGD)	−0.627	0.338	1.208
LD3 (LGD)	−0.962	0.0180	0.903
LD4 (LGD)	−0.924	0.0561	0.942

TABLE 10
$\tilde{\sigma}_{11}$ in the center of the plate with 50 × 1 mesh - Problem I

	top	middle	bottom
3D Pagano	18.81	0.09762	−18.10
LD1 (LGR)	16.50	0.1021	−15.92
LD2 (LGR)	18.53	0.09724	−17.80
LD3 (LGR)	18.80	0.09708	−18.09
LD4 (LGR)	18.81	0.09666	−18.09
LD1 (LGD)	16.50	0.1021	−15.92
LD2 (LGD)	18.53	0.09724	−17.80
LD3 (LGD)	18.80	0.09708	−18.09
LD4 (LGD)	18.81	0.09666	−18.09

TABLE 11
Undamped natural frequencies $\omega_{(m,n)}$ with m, n = number of half-waves in the plane x and y directions. (*) The free vibration frequencies are computed on the basis of homogeneous isotropic thin plate theory - Problem II

frequency modes $\omega_{(m,n)}$	(1, 1)	(2, 1)	(1, 2)	(2, 2)
Analytical values* [31]				
	39.7	98.2	98.2	157.2
Q4, 8 × 8				
LD1 (LGR)	40.1	104.9	104.9	168.9
LD1 (LGD)	40.1	104.9	104.9	168.9
LD2 (LGR)	40.1	105.6	105.6	169.7
LD2 (LGR)	40.1	105.6	105.6	169.7
LD3 (LGR)	40.1	105.6	105.6	169.7
LD3 (LGR)	40.1	105.6	105.6	169.7
LD4 (LGR)	40.1	105.6	105.6	169.7
LD4 (LGR)	40.1	105.6	105.6	169.7
Q4, 10 × 10				
LD1 (LGR)	39.8	102.5	102.5	164.7
LD1 (LGD)	39.8	102.5	102.5	164.7
Q4, 12 × 12				
LD1 (LGR)	39.7	101.3	101.3	162.4
LD1 (LGD)	39.7	101.3	101.3	162.4

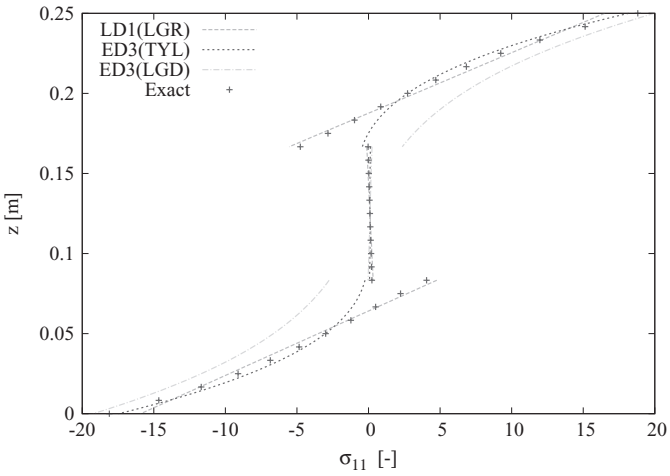

FIG. 16. Comparison between ED3 and LD1 theories with the same nDOFs: $\tilde{\sigma}_{11}$ quantity $\tilde{u}_1$-Problem I.

TABLE 12
Undamped natural frequencies in dimensionless form: $\tilde{\omega} = \omega h\sqrt{\rho/E_T}$ - Problem IV

N_l	2		3
E_L/E_T	3	30	3
Analytical [29]			
3D Exact	0.2392	0.3117	0.2516
LD4	0.2392	0.3117	0.2516
LD3	0.2392	0.3117	0.2516
LD2	0.2395	0.3168	0.2517
LD1	0.2478	0.3210	0.2556
Q9, 3 × 3			
LD4 (LGR)	0.2396	0.3121	0.2520
LD3 (LGR)	0.2396	0.3122	0.2520
LD2 (LGR)	0.2399	0.3172	0.2521
LD1 (LGR)	0.2482	0.3214	0.2560
LD4 (LGD)	0.2396	0.3121	0.2520
LD3 (LGD)	0.2396	0.3122	0.2520
LD2 (LGD)	0.2399	0.3172	0.2521
LD1 (LGD)	0.2482	0.3214	0.2560
Q9, 6 × 6			
LD3 (LGR)	0.2392	0.3118	0.2516
LD3 (LGD)	0.2392	0.3118	0.2516

TABLE 13
DOFs for Problem I with a Q4 50 × 1 mesh

Order	1	2	3	4
DOF LD	**1224**	2142	3060	3978
DOF ED	612	918	**1224**	1530

TABLE 14
Comparison between different FE models with same nDOFs: $\tilde{u}_1$ quantity - Problem I

	top	1st interface	2nd interface	bottom
Pagano Exact	−0.940	0.253	−0.201	0.920
LD1 (LGR)	−0.740	0.383	−0.149	0.902
ED3 (TYL)	−0.924	0.0190	0.00475	0.874
ED3 (LGR)	−1.269	−0.381	−0.127	0.704
ED3 (LGD)	−0.867	0.0212	0.276	1.107

TABLE 15
Comparison of different FE models with same nDOFs: $\tilde{\sigma}_{11}$ quantity - Problem I

	top	1st interface top/bottom	2nd interface top/bottom	bottom
Pagano Exact	18.81	−4.762/−0.026	0.237/4.058	−18.10
LDl (LGR)	16.50	−5.547/−0.121	0.325/4.767	−15.92
ED3 (TYL)	18.17	−0.432/0.133	0.0708/−0.2438	−17.47
ED3 (LGR)	19.97	2.357/0.248	−0.0315/−2.752	−19.24
ED3 (LGD)	19.97	2.357/0.248	−0.0315/−2.752	−19.24

Table 13 shows the number of degrees of freedom (nDOFs) related to various theories when they are employed to model the bending of the three-layered plate of problem I (with a 50×1 mesh of Q4 FEs). EDI cases correspond to the most available plate/shell elements available in commercial codes. The LD4 analysis requires more than 6 times the nDOFs considered in the EDI analysis. It is significant to notice that the third order ESL analysis (EDS) requires the same nDOFs of the first order LW analysis (LD1) (see Tab. 13). Obviously, such an equivalence is due to the considered lay-out, which consistes of a three-layered plate. LD1 becomes more expensive, or more convenient, by incerasing/reducing the number of constituent layers, respectively. An extensive comparison between LD1 and EDS results is therefore proposed in the following.

In-plane displacement results are compared in Tab. 14 while in-plane normal stresses are compared in Tab. 15. The comparison between $\tilde{u}_1$ and for $\tilde{\sigma}_{11}$ quantities is given in Figs. 15, 16. It can be stated that the LW analysis would seem to be preferable to the ESL ones herein discussed.

CONCLUSIONS

The paper has proposed a family of new FEs for multilayered plate analyses which employ Lagrangian and Legendre polynomials for the two-dimensional assumption in the thickness plate directions. These have been developed in both ESL and LW variable description frameworks. Particular emphasis has been devoted to the comparison between the proposed advanced FEs and the classical FE ones based on Taylor-type expansion in the framework of the ESL theory (which correspond to the ones available in commercial codes). The following conclusions can be made.

1. The implemented FEs have the same convergency rate as classical higher order elements for multi-layered structures.
2. The accuracy of various FEs is very much subordinate to the z-position of the evaluated variable through the thickness plate direction.
3. LW analyses are the only ones that are able to describe 3D stress-strain states in laminated structures.
4. As far as computational effort is concerned, linear LW descriptions seem to be preferable to higher order ESL theories.

The potential advantage of using Lagrange polynomials has been highlighted since they only have physical displacements as DOFs. Such an advantage could be particularly significant in nonlinear analysis since the related FEs lead to the zero-strain condition in the case of rigid body motion.

REFERENCES

1. H.G. Allen, Analysis and Design of Structural Sandwich Panels, Pergamon, 1969.
2. E.A. Thornton, Thermal Structures for Aerospace Applications, AIAA Education Series, 1996.
3. W.S. Tsai, Introduction to Composite Materials, CRC Press, 1980.
4. A.V. Srinivasan, D. Michael McFarland, Smart Structures: Analysis and Design, Cambridge University Press, 2001.
5. B. Bhushan, Springer Handbook of Nanotechnology, Springer, 2007.
6. E. Carrera, C_z^0 Requirements - Models for the Two Dimensional Analysis of Multilayered Structures, Composite Structures, vol. 37, pp. 373–383, 1997.
7. Jones, Mechanics of Composite Materials, Taylor & Francis, 1998.
8. J.N. Reddy, Mechanics of Laminated Composite Plates and Shells, Theory and Analysis, CRC Press, 1999.
9. V.V. Novozhilov, Thin Shell Theory, J.R.M. Radok, 1964.
10. E. Carrera, C_z^0 Reissner-Mindlin Multilayered Plate Elements Including zig-zag and Interlaminar Stresses Continuity, International Journal Numerical Methods in Engineering, vol. 39, pp. 1797–1820, 1996.
11. E. Carrera, Theories and Finite Elements for Multilayered Anisotropic, Composite Plates and Shells, Archives of Computational Method in Engineering, state of the art Reviews, vol. 9, pp. 87–140, 2002.
12. E. Carrera, Theories and Finite Elements for Multilayered Plates and Shells: A Unified Compact Formulation with Numerical Assessment and Benchmarking, Archives of Computational Method in Engineering, vol. 10(3), pp. 215–296, 2003.
13. B.N. Pandya, T. Kant, Flexure Analysis of Laminated Composites Using Refined Higher-Order Co Plate Bending Elements, Computer Methods in Applied Mechanics and Engineering, vol. 66, pp. 173–198, 1988.
14. T. Kant, Mallikarjuna, Vibrations of Unsymmetrically Laminated Plates Analyzed by Using a Higher-Order Theory with a cq Finite Element Formulation, Journal of Sound and Vibration, vol. 134(1), pp. 1–16, 1989.
15. K. Rohwer, Application of Higher Order Theories to the Bending Analysis of Layered Composite Plates, International Journal of Solids and Structures, vol. 29(1), pp. 105–119, 1992.

Downloaded By: [Nali, Pietro] At: 11:45 8 November 2010

16. T. Kant, K. Swaminathan, Analytical Solutions for the Static Analysis of Laminated Composite and Sandwich Plates Based on a Higher Order Refined Theory, Composite Structures, vol. 56, pp. 329–344, 2002.
17. B.N. Pandya, T. Kant, Higher-Order Shear Deformable Theories for Flexure of Sandwich Plates: Finite Element Evaluations, International Journal of Solids and Structures, vol. 24(12), pp. 1267–1286, 1988.
18. T. Kant, K. Swaminathan, Free Vibration of Isotropic, Orthotropic, and Multilayer Plates Based on Higher Order Refined Theories, Journal of Sound and Vibration, vol. 241(2), pp. 319–327, 2001.
19. E. Carrera, Historical Review of zig-zag Theories for Multilayered Plates and Shells, Applied Mechanics Review, vol. 56, pp. 287–308, 2003.
20. E.I. Grigolyuk, G.M. Kulikov, General Directions of the Development of Theory of Shells, Mekhanica Kompozitnykh Materialov, vol. 24, pp. 287–298, 1988.
21. G.M. Kulikov, E. Carrera, Finite Rotation Higher-Order Shell Models and Rigid-Body Motions, International Journal of Solids and Structures, vol. 45, pp. 3153–3172, 2008.
22. E.Carrera, Evaluation of Layer-Wise Mixed Theories for Laminated Plates Analysis, AIAA Journal, vol. 58, 36, pp. 830–839, 1998.
23. E. Carrera, L. De Masi, Classical and Advanced Multilayered Plate Elements Based Upon pvd and rmvt. Part 1. Derivation of Finite Element Matrice, International Journal Numerical Methods in Engineering, vol. 55, pp. 191–231, 2002.
24. E. Carrera, L. De Masi, Classical and Advanced Multilayered Plate Elements Based Upon pvd and rmvt. Part 2. Numerical Implementations, International Journal Numerical Methods in Engineering, vol. 55, pp. 253–291, 2002.
25. E. Carrera, Multilayered Shell Theories Accounting for Layerwise Mixed Description, Part 1: Governing Equations; Part 2: Numerical Evaluations, AIAA Journal, vol. 37(9), pp. 1107–1124, 1999.
26. E. Carrera, Theories and Finite Elements for Multilayered Plates and Shells: A Unified Compact Formulation with Numerical Assessment and Benchmarking, Archives of Computational Methods in Engineering, vol. 10, pp. 215–297, 2003.
27. E. Carrera, S. Brischetto, P. Nali, Variational Statements and Computational Models for Multifield Problems and Multilayered Structures, Special Issue of MAMS, vol. 15(3), pp. 182–198, 2008.
28. N.J. Pagano, Exact Solutions for Composite Laminates in Cylindrical Bending, J. Composite Materials, Journal of Composite Materials, vol. 3, pp. 398–411, 1969.
29. E. Carrera, An Assessment of Mixed and Classical Theories on Global and Local Response of Multilayered, Orthotropic Plates, Composite Structures, vol. 50, pp. 183–198, 2000.
30. O.C. Zienkiewicz, The Finite Element Method for Solid and Structural Mechanics, Elsevier, 2005.
31. D.J. Gorman, Free Vibration Analysis of Rectangular Plates, Elsevier, 1982.
32. G.J. Turvey, N. Mulcahy, M.B. Widden, Experimental and Computed Natural Frequencies of Square Pultruded grp Plates: Effects of Anisotropy, Hole Size Ratio and Edge Support Conditions, Composite Structures, vol. 50, pp. 391–403, 2000.

Downloaded By: [Nali, Pietro] At: 11:45 8 November 2010